06

Structure of copper centers in zeolite-mordenite at the activation stage according to XAFS and computer modelling data

© G.B. Sukharina, Ya.N. Gladchenko-Djevelekis, A.M. Ermakova, K.D. Kulaev, V.V. Pryadchenko, E.E. Ponosova, A.S. Babayants, L.A. Avakyan, L.A. Bugaev

Southern Federal University, Rostov-on-Don, Russia
e-mail: gbsukharina@sfedu.ru, ygl@sfedu.ru

Received November 6, 2024
Revised February 6, 2025
Accepted February 11, 2025

The results of the investigation on the local structure of copper centers in mordenite-type zeolites obtained by solid-phase ion exchange were presented. The location of probable models of copper centers in the mordenite-type zeolite framework for the most significant stage of the catalytic cycle, oxygen activation, was established and the features of 3*D*-models of the copper's near environment at the studied stage of the catalytic cycle were determined using a complex technique combining computer modelling with machine learning elements and X-ray absorption spectroscopy XAFS.

Keywords: zeolites, copper centers, oxygen activation, XAFS, computer modelling, DFT.

DOI: 10.61011/TP.2025.06.61377.404-24

Introduction

Zeolites are a family of microporous crystalline aluminosilicate materials containing silicon, aluminum, and oxygen atoms [1,2]. Compounds of this type are found in nature, but can also be produced synthetically [3]. Zeolites have a porous structure and can function as molecular sieves, selectively adsorbing and separating molecules of various sizes, shapes, and polarities, as well as catalyzing processes that require separation of the reaction components [4–6]. Due to their exceptional catalytic activity and wide possibilities for modifications, zeolites are used in a large number of industrial fields: as catalysts in the oil refining and chemical industries, separation and purification of gas mixtures, water purification, as well as in solar energy and as hemostatic agents in medicine [3,7–9]. To increase the catalytic activity, zeolites can be modified using heavy and transition metal atoms such as Zn, Pb, Cu, Co, Fe, etc. Such a modification may improve the reactivity of zeolites by increasing their specific surface area and porosity [10].

The focus of this work is on zeolites, which are used in C1-chemistry — a field of science that studies the catalytic transformation of molecules with one carbon atom, including CO, CO_2, CH_4, CH_3OH and HCOOH [11,12]. C1-chemistry studies the possibilities of efficient and environmentally friendly synthesis of hydrocarbons and oxygenates from simple organic molecules, and zeolites, as effective catalysts, are widely studied in this area [13]. One of the most widely studied processes in C1-chemistry is the transformation of CH_4, which is formed during natural gas extraction and decomposition of household waste and can be used in the oil industry [14–16]. The key problem of chemical transformation of methane lies in the strong bond C−H with the bond dissociation energy of 435 kJ/mol, which creates a large energy barrier for reactions and requires the use of selective and effective catalysts such as zeolites [17–19]. In our work, we consider a copper-containing zeolite–mordenite (Cu−MOR), structurally consisting of octal and duodecimal annular channels — 8 and 12, which run parallel to each other. Between the unidirectional channels are „side pockets", which are enclosed in two octal rings — 8.8 and 8.12 (the rings were named according to the nomenclature described in [20]). This type of zeolite is much more effective in catalytic oxidation of methane to methanol in terms of the resulting moles of CH_3OH per mole of copper used compared to other zeolites such as MFI, CHA and FER [17,21,22]. The catalytic properties of zeolites are largely determined by the structure of metal centers, which transforms at various stages of the catalytic cycle, one of the significant stages of which is oxygen activation.

In our previous studies [23–25] in order to determine the structure of mordenite type copper zeolite centers formed during solid-phase synthesis in the temperature range from 300 °to 400 °C, we have successfully used an approach that includes a set of traditional methods such as X-ray absorption spectroscopy and computer modeling using DFT (Density Functional Theory) [26] calculations. This approach is effective, but energy-intensive and time-consuming, and today it is required to speed up the process of obtaining information about the structure and its relationship with the properties of new catalysts.

In this work, to solve the complex problem of finding the local structure of zeolites copper centers during oxygen activation, an approach was used to analyze X-ray absorption spectra (XAFS) *in situ*, which is based on the methodology proposed by us in [20] to determine the location of the most likely copper centers in the zeolite

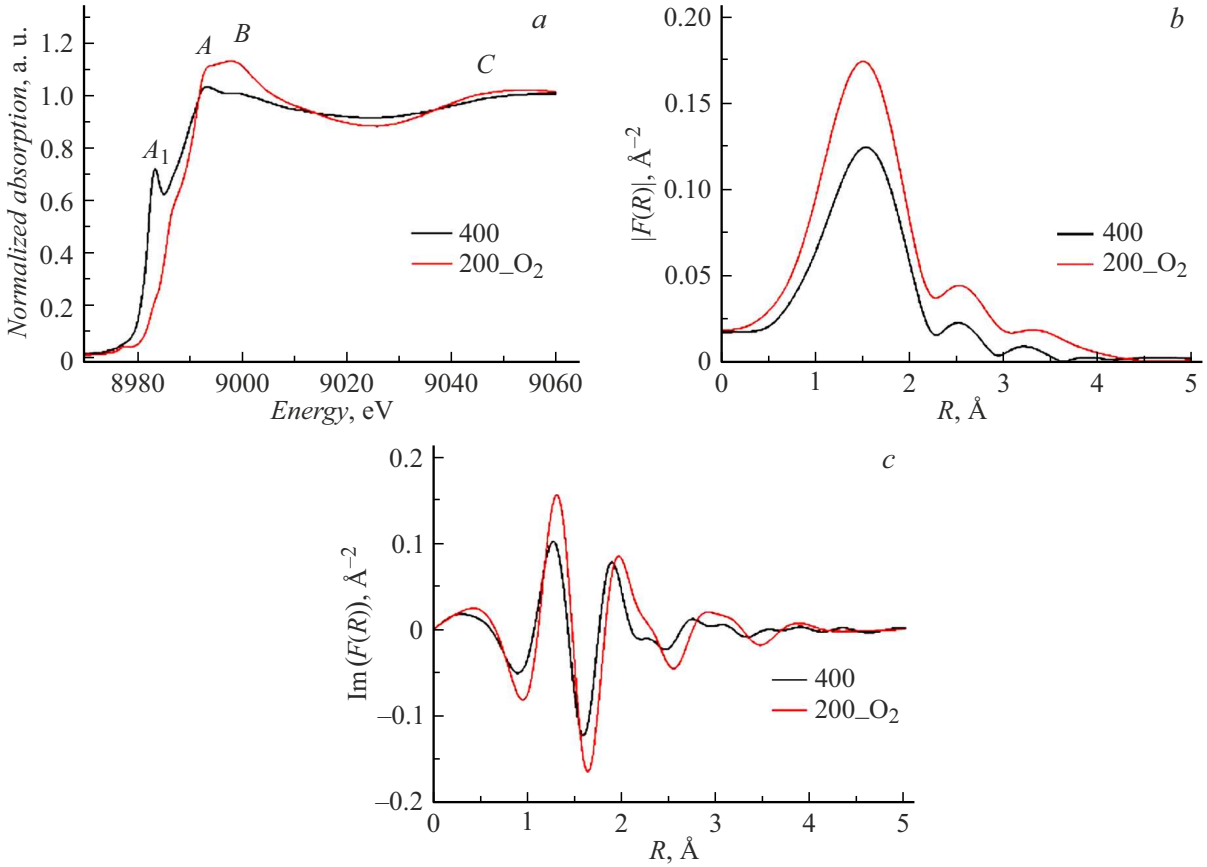

Figure 1. Comparison of experimental Cu *K*-XANES (*a*), Fourier transformation modules|F(R)| (FT-Fourier transform) (*b*) and imaginary parts Im($F(R)$) — (*c*) oscillating part $\chi(k)$ of EXAFS spectra in Cu−MOR$_{TF}$ zeolite measured during the solid-phase synthesis at a temperature of 400 °C and at the stage of oxygen activation (O_2).

carcass from the experimental data XANES using machine learning algorithms.

1. Experimental and theoretical methods

The samples of copper-containing zeolite of mordenite type considered in this work were obtained by solid-phase synthesis — Cu−MOR$_{TF}$ (Si/Al = 8.5, Cu/Al = 0.30), described in detail in [27]. For synthesis, a mixture of H−MOR (zeolite of mordenite type) and CuCl crushed in a mortar in an argon atmosphere was used; 15 mg of this mixture was fixed in a thin-walled quartz capillary, then heated from room temperature to 120 °C in flowing dry helium. To remove the water, captured in zeolite, the gas flow was stopped, and the mixture stayed in vacuum during 1 h, after which the heating in helium flow continued with a speed of 1 °C/min to 400 °C. Solid state reaction at temperature 400 °C lasted for 4 h. Then, cooling was carried out to 200 °C and O_2 was introduced for activation.

XAFS X-ray absorption spectroscopy and computer modeling with machine learning elements were used to study the structure of copper active centers at the oxygen activation stage. XAFS X-ray absorption spectra beyond *K*-copper edge were measured at Paul Scherrer Institute in Villigen (Switzerland) on SuperXAS line of a Swiss synchrotron radiation source with a beam energy of 2.4GeV and a current of 400mA. X-ray absorption spectra were obtained *in situ* conditions in a „passage through“ mode using a double-crystal monochromator Si(111). The obtained spectra were processed in IFEFFIT software [28].

The X-ray absorption spectra of Cu *K*-XANES Cu−MOR$_{TF}$ were obtained by the finite difference method in FDMNES software [29]. In modeling Cu *K*-XANES by the finite difference method for the structures of copper centers in Cu−MOR the following calculation parameters were used: — 0.5 eV up to 10 eV, 1 eV up to 20 eV and 3 eV up to 80 eV after the absorption edge, sphere radius for calculation — 6 Å. The arctangent model with standard default parameters was used for spectrum blurring when calculating in FDMNES [29] program. DFT-calculations were performed in Quantum Espresso [30] program using the exchange-correlation potential PBE for a mordenite zeolite carcass cell with a size of $1 \times 1 \times 2$ containing 288 atoms, which turned out to be sufficient to reproduce all the main spectral features of Cu *K*-XANES of the spectrum.

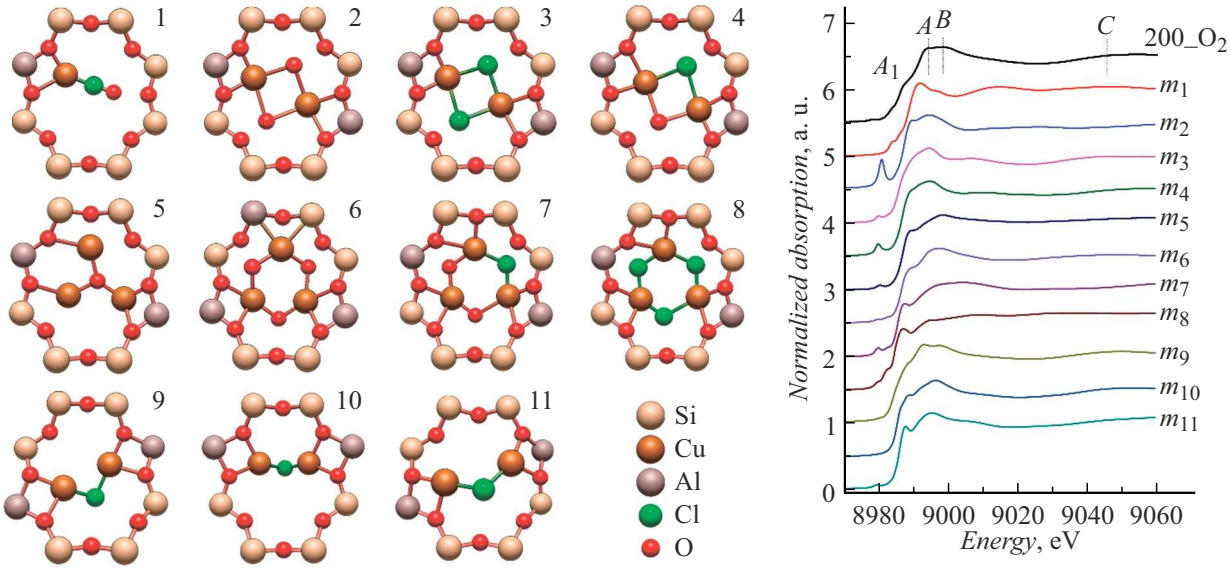

Figure 2. A set of possible structural models of copper centers considered as probable for the oxygen activation stage, and calculated Cu *K*-XANES spectra in FDMNES software corresponding to the presented models.

2. Results and discussion

In this paper, we tested the proposed [20] approach, which allows us to determine the location of the most likely copper centers characteristic of the considered stages of the catalytic cycle using computer modeling with elements of machine learning based on experimental XAFS data. The results of XAFS spectroscopy include the analysis of experimental Cu*K*-XANES/EXAFS spectra in Cu−MOR_{TF} obtained at one of the most significant stages of the catalytic cycle- oxygen activation(O_2), followed by interaction with methane (CH_4) and then directly extraction of methanol.

As seen from Fig. 1, the form Cu of *K*-XANES spectrum in Cu−MOR_{TF}, corresponding to the oxygen activation stage (O_2) is featuring specific features — pre-edge (A_1), peaks *A*, *B* and *C*. At the same time, compared to experimental Cu *K*-XANES, which characterizes the near environment of copper formed during solid-phase synthesis at a temperature of 400 ° C, a transformation of the marginal feature of A_1 is noticeable, as well as a significant change in the shape of the main maximum, namely, the increase in the intensity of the peak *A* and the formation of the peak *B*. Moreover, a change in the modules of Fourier transforms |F(R)| of extended energy areas (EXAFS) was observed for experimental Cu *K*-XAFS-spectra in Cu−MOR_{TF} zeolites. Fourier functions $F(R)$ of the oscillating part of $\chi(k)$ (k, wavenumbers of photoelectrons) of experimental spectrum Cu *K*-EXAFS are given for the range Δk from 3 to 8 $Å^{-1}$. This behavior of experimental spectra indicates a change in the near environment of copper in the zeolite at the stage of oxygen activation (O_2) compared with the previous stage of solid-phase synthesis at a temperature of 400 ° C. To determine the structure of copper centers at this stage of catalytic cycle, we tested a technique that is a combination of machine learning methods and X-ray absorption spectroscopy, which we proposed in our work [20]. In this study we used a fully-connected neural network based on the modules of pytorch [31] library and trained using a training set of synthetic data — Cu *K*-XANES spectra calculated in FDMNES software for more than 14 000 models of copper centers given the presence of CuO and Cu_2O oxides. The machine learning algorithms used are able to determine the location of the copper center in the zeolite ring with an accuracy of 0.97 according to F1 metric. Thus, as a first approximation to determine the most probable copper environment in the zeolite carcass corresponding to the oxygen activation stage, using the methodology proposed in [20], the location of copper centers in a specific structural ring was determined. Further, taking into account the obtained structural information and literature data from [23,32,33], eleven most probable variants of copper centers were modeled (Fig. 2), for each of which Cu*K*-XANES spectrum was calculated. Table 1 gives the residual values (Δ) for experimental and theoretical Cu *K*-XANES in Cu−MOR_{TF} calculated for eleven considered models of copper centers at the stage of oxygen activation.

Table 1. Quantitative characterization of the correspondence of the proposed models of copper centers to experimental data of Cu *K*-XANES in Cu−MOR_{TF} at the oxygen activation stage

Mean-square error (Δ)										
m_1	m_2	m_3	m_4	m_5	m_6	m_7	m_8	m_9	m_{10}	m_{11}
0.11	0.10	0.07	0.08	0.09	0.05	0.10	0.16	0.07	0.07	0.07

The residual error is a value determined using a mean-square error between the simulated and experimental Cu

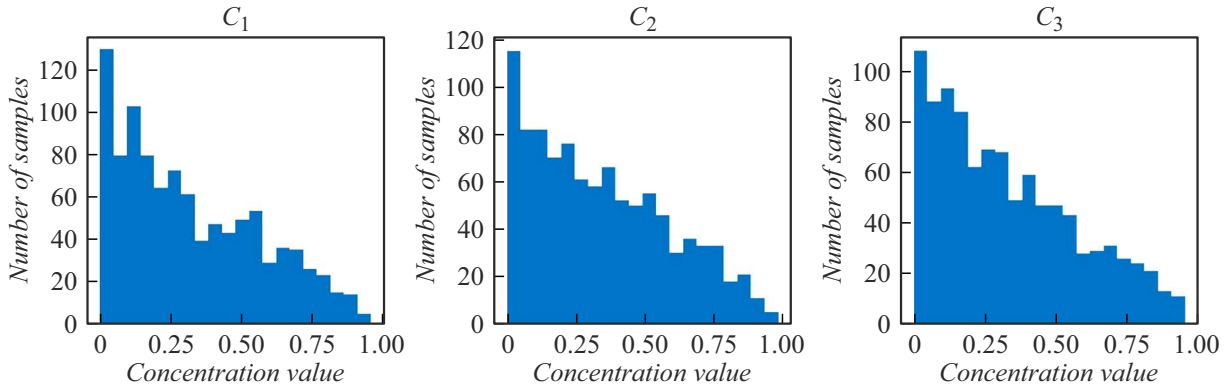

Figure 3. Visual representation of Dirichlet distribution for coefficients characterizing the contributions from two different models of copper centers and copper oxide.

Table 2. Quantitative characterization of the reliability of the considered coatings of the near environment of Cu atoms in zeolite Cu−MOR_{TF}, taking into account contributions from various copper centers characteristic of the oxygen activation stage

Contribution	Mean-square error (Δ)				
	LCM-1	LCM-2	LCM-3	LCM-4	LCM-5
before optimization	0.037	0.075	0.057	0.097	0.033
after optimization	0.100	0.040	0.037	0.055	0.003

K-XANES spectra in Cu−MOR_{TF} according to the following formula:

$$\Delta = \left[\frac{1}{E_2 - E_1} \int_{E_1}^{E_2} (\mu(E) - \mu_{\exp}(E))^2 \, dE \right]^{\frac{1}{2}},$$

where $\mu(E)$ — theoretical spectrum, $\mu_{\exp}(E)$ — experimental spectrum, E_1 and E_2 — limits of energy interval.

The energy interval 8969−9059 eV, corresponding to the appropriate XANES spectra was used to calculate the residual error. As can be seen from Table 1, the best consistency with the experiment is demonstrated by the theoretical spectra calculated for the models m_3, m_6, m_9, m_{10} and m_{11}. However, none of these models allowed reproducing all the features of the experimental Cu*K*-XANES spectrum (Fig. 2). Since XAFS contains averaged information about the local atomic structure for a certain type of atom across the sample, in order to comply with the experiment, it is necessary to allow for the contributions to the theoretical Cu*K*-XANES from several probable copper centers peculiar to the oxygen activation stage. Also, it should be taken into account that at the stage of oxygen activation some copper oxides like CuO and Cu_2O may make some contribution to Cu *K*-XANES spectrum. To automatically determine the contributions of each of the considered models of the copper center and the corresponding oxide (CuO and Cu_2O), an algorithm

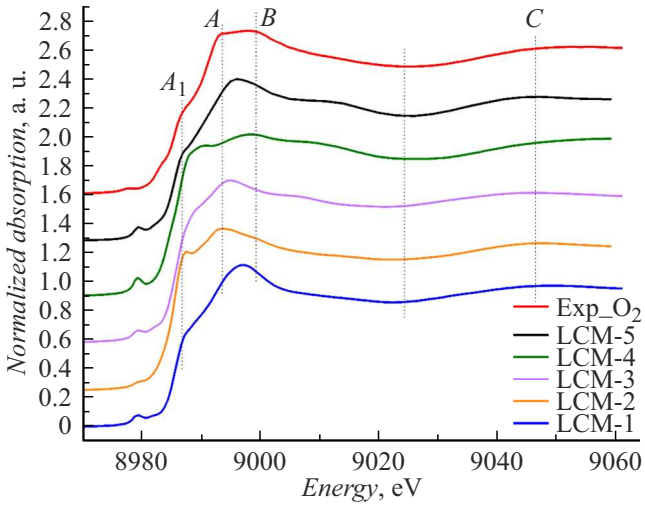

Figure 4. Experimental and theoretical Cu *K*-XANES in Cu−MOR_{TF}calculated for the considered LCM before optimizing the geometry of structural models of copper centers, presumably corresponding to the near environment of copper at the stage of oxygen activation.

for selecting coefficients responsible for the magnitude of the contribution from a particular model of the copper center was written in Python. Using Dirichlet function from numpy [34] library (Fig. 3) was formed with parameters $\alpha = [0.9, 0.9, 0.9]$ as a matrix of weight coefficients 3×1000.

The sum of each row of such a matrix was one. For each combination of coefficients, models of copper centers were found by iteration, allowing us to obtain the smallest residual error between the experimental and theoretical Cu *K*-XANES spectra. For example, quantitative characteristics of the quality of consistency between experimental and theoretical Cu are given in Table 2. *K*-XANES of the spectrum corresponding to different combinations of coefficients taking into account the contributions from the determined most probable m_3, m_6, m_9, m_{10} and m_{11} models of the copper centers and one of the considered copper oxides CuO

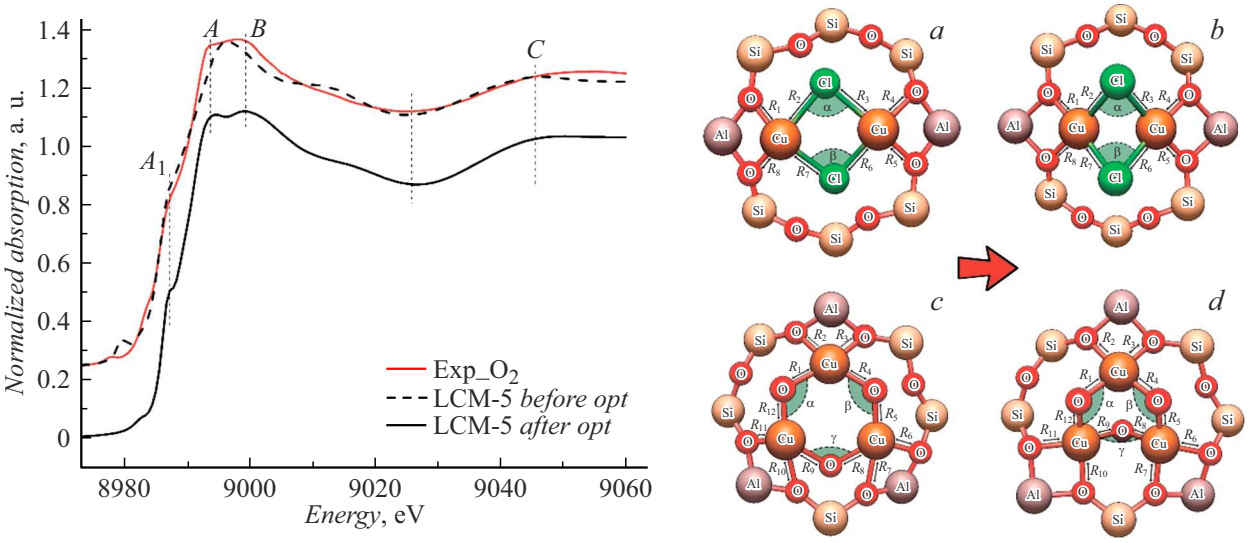

Figure 5. Comparison of experimental and theoretical Cu*K*-XANES in Cu−MOR$_{TF}$for the oxygen activation stage corresponding to LCM-5, taking into account contributions from the most probable models of copper centers, and visualization of their structures before and after improvement of their geometry in Quantum Espresso software: m_3 (a, b) and m_6 (c, d).

Table 3. Structural parameters obtained as a result of geometry improvement for the copper center model–m_3, characteristic of the oxygen activation stage in Cu−MOR$_{TF}$

Cu−O	Cu−Cl	Cu−Cl	Cu−O	Cu−Al	Cu−Cl−Cu
$R \pm 0.01$ (Å)					angle ±1°
$R_1 = R_5$	$R_2 = R_6$	$R_3 = R_7$	$R_4 = R_8$	R	$\alpha = \beta$
1.98	2.24	2.21	2.04	2.80	74

or Cu_2O. Thus, the following linear combinations (LCM) are considered, taking into account the contributions from various most probable models of the copper environment with the corresponding coefficients C_1, C_2 and C_3: LCM-1 with coefficients $C_1 = 0.7$ and $C_2 = 0.3$, taking into account the contributions from the copper center m_6 and CuO oxide; LCM-2 — $C_1 = 0.4$, $C_2 = 0.4$ and $C_3 = 0.2$, contributions from models m_{11}, m_9 and Cu_2O oxide; LCM-3 — $C_1 = 0.7$, $C_2 = 0.2$ and $C_3 = 0.1$, contributions from models m_3, m_6 and Cu_2O oxide; LCM-4 — $C_1 = 0.6$, $C_2 = 0.3$ and $C_3 = 0.1$, contributions from models m_{10}, m_9 and Cu_2O oxide; LCM-5 — $C_1 = 0.7$, $C_2 = 0.2$ and $C_3 = 0.1$, contribution from models m_3, m_6 and Cu_2O oxide.

Figure 4 shows a comparison of the experimental and calculated Cu *K*-XANES in Cu−MOR$_{TF}$ corresponding to the considered LCM, presumably characterizing the local atomic structure of the copper's closest environment during oxygen activation. A set of qualitative and quantitative estimates of experimental and theoretical Cu *K*-XANES in Cu−MOR$_{TF}$, presented in Fig. 4 and in Table 2 allows to identify LCM-5 as the most probable one characterizing the copper's nearest environment during oxygen activation.

As can be seen in Fig. 4, the found combination of coefficients corresponding to LCM-5 allows us to reproduce the main trends of experimental Cu *K*-XANES corresponding to the oxygen activation stage, however, in the region of the main maximum of the characteristic *A* and *B*, as well as in the energy range from 9008 to 9018 eV, there is a slight discrepancy between theoretical and experimental spectra. The improvement of geometry of the structural models m_3 and m_6 (LCM-5) performed in Quantum Espresso software made it possible to minimize the observed discrepancies between the experimental and theoretical Cu*K*-XANES spectra corresponding to the nearest environment of copper at the stage of oxygen activation, and to reproduce all the main spectral features in the experiment. Thus, it was found that if taking into account the contributions of the copper centers models m_3, m_6 and Cu_2O oxide with the corresponding coefficients $C_1 = 0.7$, $C_2 = 0.2$ and $C_3 = 0.1$ we may achieve the consistency between theoretical and experimental data (Fig. 5). The mean-square error for the obtained LCM-5 was 0.003, which is an order of magnitude less than all the other LCM considered by us, taking into account contributions from other types of copper centers. Table 3 and 4 provides a full 3*D*-geometry of the obtained structural models of the copper centers m_3 and m_6 — interatomic distances and bond angles.

Thus, it was found that the copper centers m_3 and m_6 (Fig. 5), characteristic of the oxygen activation stage, are located in the structural ring — 8.12 of the mordenite zeolite carcass. The obtained models m_3 and m_6 represent two-copper and three-copper centers where either two oxygen atoms and two chlorine atoms or four oxygen atoms are located in the nearest environment of copper, respectively.

Table 4. Structural parameters obtained as a result of geometry improvement for the copper center model–m_6, characteristic of the oxygen activation stage in Cu−MOR_{TF}

Cu−O	Cu−CO	Cu−CO	Cu−O	Cu−O	Cu−Al	Cu−O−Cu
$R \pm 0.01$ (Å)						angle ±1°
$R_1 = R_5 = R_8 = R_9 = R_{12}$	$R_3 = R_{11}$	$R_2 = R_7 = R_{10}$	R_4	R_6	R	$\alpha = \beta = \gamma$
1.77	1.91	1.95	1.81	1.99	2.77(1) 2.72(2)	112

Conclusion

An approach is proposed that allows using a combination of computer modeling methods with machine learning elements and X-ray absorption spectroscopy to solve the problem of determining the most likely structures of copper zeolite centers that transform at various stages of the catalytic cycle. The difficulty of determining the structural models of the copper environment using only traditional approaches such as XANES or EXAFS is due to the presence of various types of copper centers in zeolite carcass, since such methods allow obtaining average structural information. However, using the proposed approach, it was possible to determine a probable model of the nearest environment of copper atoms in Cu−MOR_{TF}, which is specific for the most significant stage of the catalytic cycle —oxygen activation. It was found that theoretical linear combination (LCM-5), corresponding to the nearest environment of copper in the zeolite-mordenite carcass during oxygen activation, contains contributions from Cu_2O oxide, as well as from copper centers m_3 and m_6. The structural characterization of the obtained models is performed, the structural parameters of the interatomic distances and bond angles for both types of copper centers are determined. Thus, this technique has proven to be an effective tool for determining the structure of copper centers of mordenite-type zeolites relatively quickly compared to conventional approaches. In the future, the study of such porous materials, in particular other types of zeolites, using the proposed methodology requires its improvement and generalization.

Funding

This study was supported by grant No. 23-22-00438 from the Russian Science Foundation, https://rscf.ru/project/23-22-00438/ in the Southern Federal University.

Acknowledgments

The authors express their gratitude to professor Yu.V. Bockhoven (Swiss Federal Institute of Chemistry and Bioengineering (ETH), as well as to V.V. Srabionyan, associate professor in SFU for their help and assistance.

Conflict of interest

The authors declare that they have no conflict of interest.

References

[1] E.M.C. Alayon, M. Nachtegaal, A. Bodi, M. Ranocchiari, J.A. van Bokhoven. Phys. Chem. Chem. Phys., **17**, 7681 (2015). https://doi.org/10.1039/C4CP03226H
[2] E.M.C. Alayon, M. Nachtegaal, E. Kleymenov, J.A. van Bokhoven. Microporous Mesoporous Mater., **166**, 131 (2013). https://doi.org/10.1016/j.micromeso.2012.04.054
[3] Y. Li, L. Li, J. Yu. Chem., **3**, 928 (2017). https://doi.org/10.1016/j.chempr.2017.10.009
[4] Y. Li, J. Yu. Nat. Rev. Mater., **6**, 1156 (2021). https://doi.org/10.1038/s41578-021-00347-3
[5] M. Moliner, C. Martinez, A. Corma. Chem. Mater., **26**, 246 (2014). https://doi.org/10.1021/cm4015095
[6] N. Rangnekar, N. Mittal, B. Elyassi, J. Caro, M. Tsapatsis. Chem. Soc. Rev., **44**, 7128 (2015). https://doi.org/10.1039/C5CS00292C
[7] T. Bein, S. Mintova. Adv. Applications Zeolites, 263 (2005). https://doi.org/10.1016/S0167-2991(05)80015-1
[8] S. Mintova, M. Jaber, V. Valtchev. Chem. Soc. Rev., **44**, 7207 (2015). https://doi.org/10.1039/C5CS00210A
[9] E.T.C. Vogt, B.M. Weckhuysen. Chem. Soc. Rev., **44**, 7342 (2015). https://doi.org/10.1039/C5CS00376H
[10] M. Senila, O. Cadar. Heliyon, **10**, e25303 (2024). https://doi.org/10.1016/j.heliyon.2024.e25303
[11] W. Zhou, K. Cheng, J. Kang, C. Zhou, V. Subramanian, Q. Zhang, Y. Wang. Chem. Soc. Rev., **48**, 3193 (2019). https://doi.org/10.1039/C8CS00502H
[12] X. Jiang, X. Nie, X. Guo, C. Song, J.G. Chen. Chem. Rev., **120**, 7984 (2020). https://doi.org/10.1021/acs.chemrev.9b00723
[13] Q. Zhang, J. Yu, A. Corma. Adv. Mater., **32**, (2020). https://doi.org/10.1002/adma.202002927
[14] M. Saunois, A.R. Stavert, B. Poulter, P. Bousquet, J.G. Canadell, R.B. Jackson, P.A. Raymond, E.J. Dlugokencky, S. Houweling, P.K. Patra, P. Ciais, V.K. Arora, D. Bastviken, P. Bergamaschi, D.R. Blake, G. Brailsford, L. Bruhwiler, K.M. Carlson, M. Carrol, S. Castaldi, N. Chandra, C. Crevoisier, P.M. Crill, K. Covey, C.L. Curry, G. Etiope, C. Frankenberg, N. Gedney, M.I. Hegglin, L. Höglund-Isaksson, G. Hugelius, M. Ishizawa, A. Ito, G. Janssens-Maenhout, K.M. Jensen, F. Joos, T. Kleinen, P.B. Krummel, R.L. Langenfelds, G.G. Laruelle, L. Liu, T. Machida,

S. Maksyutov, K.C. McDonald, J. McNorton, P.A. Miller, J.R. Melton, I. Morino, J. Müller, F. Murguia-Flores, V. Naik, Y. Niwa, S. Noce, S. O'Doherty, R.J. Parker, C. Peng, S. Peng, G.P. Peters, C. Prigent, R. Prinn, M. Ramonet, P. Regnier, W.J. Riley, J.A. Rosentreter, A. Segers, I.J. Simpson, H. Shi, S.J. Smith, L.P. Steele, B.F. Thornton, H. Tian, Y. Tohjima, F.N. Tubiello, A. Tsuruta, N. Viovy, A. Voulgarakis, T.S. Weber, M. van Weele, G.R. van der Werf, R.F. Weiss, D. Worthy, D. Wunch, Y. Yin, Y. Yoshida, W. Zhang, Z. Zhang, Y. Zhao, B. Zheng, Q. Zhu, Q. Zhu, Q. Zhuang. Earth Syst. Sci. Data, **12**, 1561 (2020). https://doi.org/10.5194/essd-12-1561-2020

[15] J.E. Rorrer, G.T. Beckham, Y. Román-Leshkov. JACS Au. **1**, 8–12 (2021). https://doi.org/10.1021/jacsau.0c00041

[16] Y. Gao, J. Jiang, Y. Meng, F. Yan, A. Aihemaiti. Energy Convers. Manag., **171**, 133 (2018). https://doi.org/10.1016/j.enconman.2018.05.083

[17] S. Prodinger, K. Kvande, B. Arstad, E. Borfecchia, P. Beato, S. Svelle. ACS Catal., **12**, 2166 (2022). https://doi.org/10.1021/acscatal.1c05091

[18] N.J. Gunsalus, A. Koppaka, S.H. Park, S.M. Bischof, B.G. Hashiguchi, R.A. Periana. Chem. Rev., **117**, 8521 (2017). https://doi.org/10.1021/acs.chemrev.6b00739

[19] M.H. Groothaert, P.J. Smeets, B.F. Sels, P.A. Jacobs, R.A. Schoonheydt. J. Am. Chem. Soc., **127**, 1394 (2005). https://doi.org/10.1021/ja047158u

[20] Ya.N. Gladchenko-Djevelekis, G.B. Sukharina, A.M. Ermakova, K.D. Kulaev, V.V. Pryadchenko, E.E. Ponosova, E.I. Shemetova, L.A. Avakyan, L.A. Bugaev. Tech. Phys. **69**, 586 (2024). https://doi.org/10.61011/JTF.2024.04.57533.287-23

[21] M.A. Newton, A.J. Knorpp, V.L. Sushkevich, D. Palagin, J.A. van Bokhoven. Chem. Soc. Rev., **49**, 1449 (2020). https://doi.org/10.1039/C7CS00709D

[22] A.J. Knorpp, M.A. Newton, S.C.M. Mizuno, J. Zhu, H. Mebrate, A.B. Pinar, J.A. van Bokhoven. Chem. Commun., **55**, 11794 (2019). https://doi.org/10.1039/C9CC05659A

[23] V.V. Srabionyan, G.B. Sukharina, T.I. Kurzina, V.A. Durymanov, A.M. Ermakova, L.A. Avakyan, E.M.C. Alayon, M. Nachtegaal, J.A. van Bokhoven, L.A. Bugaev. J. Phys. Chem. C, **125**, 25867 (2021). https://doi.org/10.1021/acs.jpcc.1c08240

[24] V.V. Pryadchenko, G.B. Sukharina, A.M. Ermakova, S.V. Bazovaya, T.I. Kurzina, V.A. Durymanov, V.A. Tolstopyatenko, V.V. Srabionyan, L.A. Avakyan, L.A. Bugaev. Tech. Phys., **66**, 1018 (2021). https://doi.org/10.1134/S1063784221070124

[25] V.V. Srabionyan, G.B. Sukharina, S.Y. Kaptelinin, V.A. Durymanov, A.M. Ermakova, T.I. Kurzina, L.A. Avakyan, L.A. Bugaev. Phys. Solid State, **62**, 1222 (2020). https://doi.org/10.1134/S1063783420070252

[26] N. Argaman, G. Makov. Am. J. Phys., **68**, 69 (2000). https://doi.org/10.1119/1.19375

[27] S.E. Bozbag, E.M.C. Alayon, J. Pech..ek, M. Nachtegaal, M. Ranocchiari, J.A. van Bokhoven. Catal. Sci. Technol., **6**, 5011 (2016). https://doi.org/10.1039/C6CY00041J

[28] B. Ravel, M. Newville. J. Synchrotron Radiat., **12**, 537 (2005). https://doi.org/10.1107/S0909049505012719

[29] Y. Joly. Phys. Rev. B, **63**, 125120 (2001). https://doi.org/10.1103/PhysRevB.63.125120

[30] P. Giannozzi, S. Baroni, N. Bonini, M. Calandra, R. Car, C. Cavazzoni, D. Ceresoli, G.L. Chiarotti, M. Cococcioni, I. Dabo, A. Dal Corso, S. de Gironcoli, S. Fabris, G. Fratesi, R. Gebauer, U. Gerstmann, C. Gougoussis, A. Kokalj, M. Lazzeri, L. Martin-Samos, N. Marzari, F. Mauri, R. Mazzarello, S. Paolini, A. Pasquarello, L. Paulatto, C. Sbraccia, S. Scandolo, G. Sclauzero, A.P. Seitsonen, A. Smogunov, P. Umari, R.M. Wentzcovitch. J. Phys. Condens. Matter., **21**, 395502 (2009). https://doi.org/10.1088/0953-8984/21/39/395502

[31] Electronic source. Available at: https://pytorch.org/

[32] M.H. Mahyuddin, T. Tanaka, A. Staykov, Y. Shiota, K. Yoshizawa. Inorg. Chem., **57**, 10146 (2018). https://doi.org/10.1021/acs.inorgchem.8b01329

[33] P. Han, Z. Zhang, Z. Chen, J. Lin, S. Wan, Y. Wang, S. Wang. Catalysts., **11**, 751 (2021). https://doi.org/10.3390/catal11060751

[34] Electronic source. Available at: https://numpy.org/

Translated by T.Zorina